

Coordinated Multipoint Trials in the Downlink

V. Jungnickel, L. Thiele, T. Wirth
T. Haustein, S. Schiffermüller, A. Forck
S. Wahls, S. Jaeckel, S. Schubert, H. Gäbler

Fraunhofer Heinrich Hertz Institute
Einsteinufer 37
10587 Berlin, Germany

C. Juchems
F. Luhn
R. Zavrtak

IAF GmbH
Berliner Str. 52j
38104 Braunschweig, Germany

H. Droste, G. Kadel
W. Kreher, J. Mueller
W. Stoermer, G. Wannemacher

Deutsche Telekom AG
Deutsche-Telekom-Allee 7
64295 Darmstadt, Germany

Abstract—Coordinated multi-point (CoMP) is a new class of transmission schemes for interference reduction in the next generation of mobile networks. We have implemented and tested a distributed CoMP transmission approach in the downlink of an LTE-Advanced trial system operating in real time over 20 MHz bandwidth. Enabling features such as network synchronization, cell- and user-specific pilots, feedback of multi-cell channel state information and synchronous data exchange between the base stations have been implemented. Interference-limited transmission experiments have been conducted using optimum combining with interference-aware link adaptation and cross-wise interference cancellation between the cells. The benefits of CoMP transmission have been studied over multi-cell channels recorded in an urban macro-cell scenario.

I. INTRODUCTION

Inter-cell interference is the limiting factor in mobile networks. Recently it was noted that generalized multiple-input multiple-output (MIMO) techniques have the potential to remove this interference [1–4]. Information theory considers a centralized network architecture where the antennas of all base stations (BSs) act as inputs of the generalized MIMO system. Over the backhaul, antennas are connected to a central unit (CU) performing joint signal processing for the terminals served in all cells. The antennas of all terminals act as outputs of the MIMO system. Perfect synchronization, unlimited backhaul and negligible delay are assumed further. By removing all interference a performance can be achieved as in an isolated cell [5].

Recent results applying generalized MIMO techniques to cellular networks show huge gains also in real propagation environments [6–9]. In the 3GPP standardization activities concerning LTE-Advanced [10], these techniques fall into the category of coordinated multi-point (CoMP) transmission and reception. They are considered as tool to improve the coverage of high data rates and the cell edge throughput. Higher complexity, growing data rates on the backhaul and additional overhead are challenges for the application of CoMP techniques, especially in the down-link.

A distributed system architecture has been suggested recently. Several methods cutting the feedback and backhaul requirements have been proposed [11–14]. In this paper we describe a first real-time implementation of distributed CoMP in the downlink. Our contribution is to provide a first proof of this concept as well as initial measurements using real-world channels.

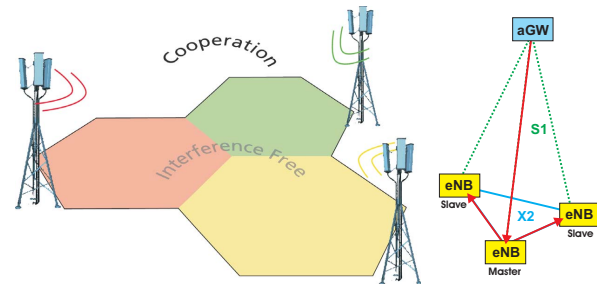


Figure 1. Using coordinated multi-point transmission, interference is removed from mobile networks. Right: Distributed mobile network architecture.

II. DISTRIBUTED CoMP NETWORK

For CoMP we need to know the down-link channel prior to the transmission. In the frequency division duplex (FDD) mode, up-link and down-link are not reciprocal. Terminals estimate the channel to the strongest base stations and provide channel state information (CSI) feedback to their serving base station (BS).

CoMP can be implemented in two ways: centralized or distributed. In the centralized CoMP transmission concept, a central unit (CU) is the genius where all CSI and data are available. The CU pre-computes all waveforms and sends them over a star-like network to the coordinated base stations acting as remote radio heads (RRHs). The centralized approach has a higher backhaul effort since IQ samples of the waveforms are transmitted. Moreover, latency requirements are tight. Waveforms must be irradiated time-aligned on a few μs timescale, i.e. within the cyclic prefix (CP). The individual propagation delay over the network requires careful compensation at each RRH.

For distributed CoMP transmission a limited set of BS transmit data jointly to multiple terminals in their cells. For each terminal, the serving BS coordinates the data flow coming from the advanced gateway (aGW) to the terminal. As a fundamental requirement of the distributed approach, BSs involved in a CoMP transmission exchange data and CSI over a meshed signaling network. Feeder and signaling interfaces at BSs are referred to as S1 and X2, respectively (Fig. 1, right). Notice that data instead of IQ samples transfer is a lighter burden for the backhaul compared to the centralized approach. Furthermore, the latency constraint can be relaxed. Waveforms are now computed locally at each base station.

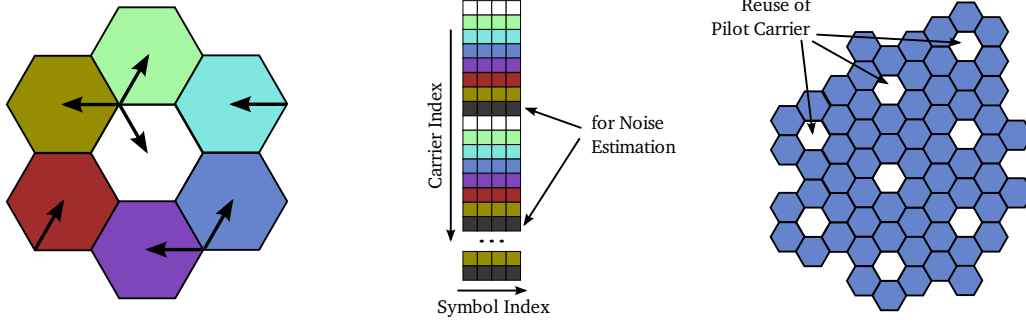


Figure 2. Design example for CSI reference signals (CSI-RS).

Provided that the data are synchronized and aging of the CSI is limited, distributed CoMP can be realized with latencies of a few ms.

Signal processing can be distributed among the BS in this network. Each BS in the cooperation cluster has the same CSI and data available and it can compute independently from other BSs the waveforms to be transmitted locally. The approach is similar to distributed beam-forming [15]. However, we need tight synchronization of the signal processing and the radio frontends at all the BSs. Last but not least each base station needs a local precoding unit, refer to section III. Inputs of the local precoder are all data streams to be processed jointly and outputs are the signals transmitted from local antennas. The distributively precoded signals combine over the air at the terminals constructively for the desired waveforms and destructively for the interference, see Fig. 3.

III. ENABLING FEATURES

A. Clock Synchronization

A first requirement of CoMP is that the physical layer and radio front-ends are tightly synchronized. A precise clock reference can be obtained from the global positioning system (GPS) at outdoor base stations. Indoor base stations can be synchronized over the network using standard protocols such as IEEE1588v2 or proprietary solutions like synchronous Ethernet [16]. From the global reference, all local clock signals needed to synchronize the radio front-end as well as frame-, symbol- and sample timing can be derived [17].

B. Synchronous Data Exchange

A second requirement is that data flows are strictly synchronized at the inputs of the local precoding unit. In the centralized approach, all data flows are terminated at the CU and thus, data synchronization is easier. In the distributed approach, such synchronization is required so that two BSs involved in a CoMP transmission transmit the same data symbol on the same resource element.

As indicated in Fig. 1 right, data are transmitted in a first hop over S1 from the aGW to the serving BS. Data are then packed into transport blocks, encoded and mapped on the resource blocks (RBs). After the MAC layer we have copied these already mapped data and forwarded the copy in a second hop over X2 to all base stations involved in the CoMP transmission (see Fig. 3). A similar data exchange is already used in LTE Rel. 8. Data still waiting in the user queue are forwarded over X2 to the next serving base station after a hard hand-over event from one cell to the next.

Compared to the centralized approach this has the advantage that data bits, and not IQ samples, are exchanged between the base stations. The load in the backhaul is significantly reduced in this way. Moreover, it is easier to synchronize the data at all BS at this stage in the transmission chain where all network and MAC layer processing is already completed. Thus, retransmissions are also controlled locally and need no additional coordination between the BS. Given that the X2 interface does not introduce to much latency, the delay due to the data exchange is easily compensated using buffers at the precoder inputs [17].

C. Cell-Specific Pilots

For the purpose of joint precoding, BSs shall provide cell-specific reference signals (RS) from which terminals can estimate the multi-cell CSI. In an orthogonal frequency division multiplexing (OFDM) based air interface, these so-called CSI reference signals (CSI-RS) can be designed in the frequency domain. According to the sampling theorem, the channel must be tested at least as often within the system bandwidth as there are independent fading taps in the time domain. The length of the cyclic prefix (CP) can be used as a lower bound for the density of pilots needed. We have used one pilot per 8 subcarriers according to the short CP in LTE.

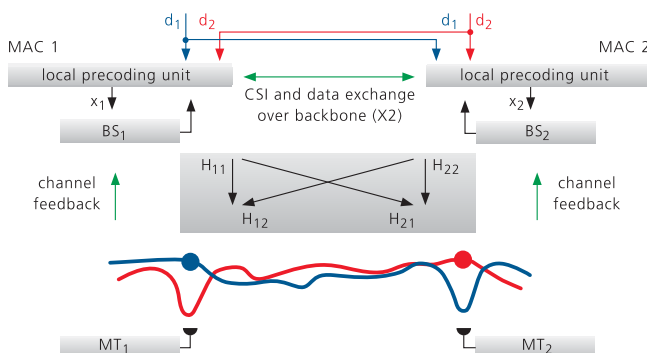


Figure 3. Distributed coordinated multi-point transmission.

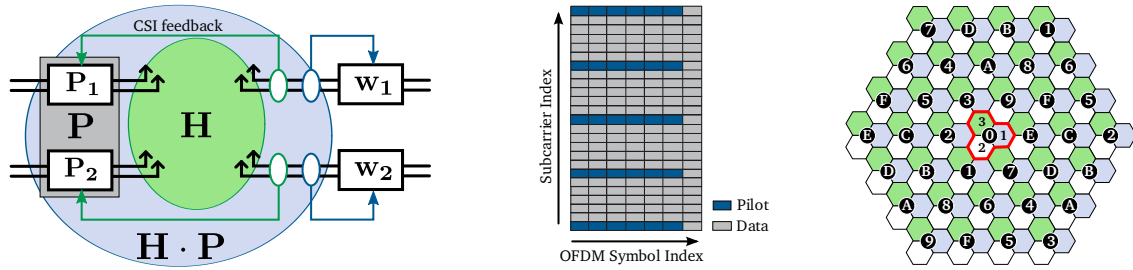


Figure 4. Design example for demodulation reference signals.

The pilot design is shown in Fig. 2. With the chosen grid spacing, 8 cells can be identified. We apply a cyclic shift of a pilot comb in the frequency domain by an integer number of subcarriers identifying the cell. Consider the elementary interference scenario in Fig. 2, left and the sequence assignment, center. If we identify each of the 7 cells by a shift from 0...6, shift 7 e.g. allows a precise noise estimation. Seven is often used as a reference for the frequency reuse factor in mobile networks (see Fig. 2, right). In a full network, we can reuse this principle and apply the same shift in the second one after the next cell. Since interference is significantly reduced now, the CSI estimation error is improved by 11 dB at the cell edge and 18 dB on average compared to full frequency reuse for the pilots normally used in LTE Release 8 [18].

D. CSI Feedback

Another requirement is that the multi-cell CSI is fed back from each terminal to the serving BS. The provision of feedback causes a significant overhead if it is not properly organized. Several techniques are known to minimize this overhead. Firstly, one may provide feedback only for RBs assigned to a user. This is suboptimal but it divides the amount of feedback provided by each terminal by the number of terminals in a cell, in case of a fully loaded cell [12].

Next one may exploit correlation in time- and frequency domains. At low mobility and in a channel with limited multipath, correlation is likely. In a scenario where demanding users are not likely to be mobile, the feedback rate can be reduced significantly. However, there is an inevitable up-link delay in the order of 5 ms for LTE. Moreover, the distribution of the CSI over the network and the computation of the precoder weights takes additional time. The overall delay calls for the use of prediction techniques [19].

E. Precoder

The local precoder is a versatile tool enabling a manifold of multi-cell transmission schemes, refer to Section V. The precoder consists of a linear matrix-vector multiplication unit. The incoming IQ signal constellations of data streams from all BSs in a CoMP transmission are multiplied with a weight matrix before the signals are passed into the IFFT at each antenna.

There is an algorithm part executed in a DSP for setting the weights. For CoMP, this algorithm assembles first the CSI received over the feedback link. The resulting channel

matrix includes all BS and all terminals involved in the CoMP transmission. Next the channel received over the uplink is interpolated in the frequency domain. For efficient methods refer to [20]. Finally, the precoding matrix is evaluated on each sub-carrier, accordingly. Hard- and software parts of the precoder interact over a memory interface.

F. Precoded Pilots

The precoding matrix \mathbf{P} depends on the CSI feedback from terminals in other cells as well. Consequently, we need a second set of pilots to estimate the precoded channel \mathbf{HP} as indicated in Fig. 4, left. \mathbf{H} is the physical channel between all transmit antennas and receive antennas at the terminal.

CSI feedback is provided sparsely in time and frequency domains. Due to the time variance of the channel precoding becomes imprecise and there is residual cross-talk from co-channel streams, served by the same CoMP transmission, or from other streams. In order to assist the demodulation at the terminal we have identified each co-channel stream according to the cell being the server for this stream by a precoded pilot sequence. These sequences are also referred to as demodulation reference signals (DM-RS) and they enable estimation of residual cross-talk and application of advanced receiver algorithms such as interference rejection combining (IRC) or successive interference cancellation (SIC). The repetition rate of the DM-RS can be higher than for the CSI-RS. Beside the cross-talk also residual phase drifts shall be removed.

The basic idea for the DM-RS design is to use the same pilots originally used without precoding and to pass them through the precoder. Unfortunately the pilot pattern used in LTE Release 8 is shifted by a cell-specific offset depending on the cell identifier. The major disadvantage is that a resource element being a known pilot in one cell carries unknown data in another cell. Due to the lack of knowledge about the random data we are unable to estimate the interference channels from other cells with similar precision as the channel in the own cell. For this purpose we have modified the original LTE pilots such that on resource elements intended for pilots no more unknown data are transmitted, cf. Fig. 4.

We use a two-step approach based on code-division multiplexing (CDM). Within a slot of 0.5 ms consisting of 7 OFDM symbols, one approach is to transmit in all cells and on the same subcarrier grid a sector-specific sequence. In deployments with two transmit antennas and three sectors per site, the sequence would last over 6 OFDM symbols.

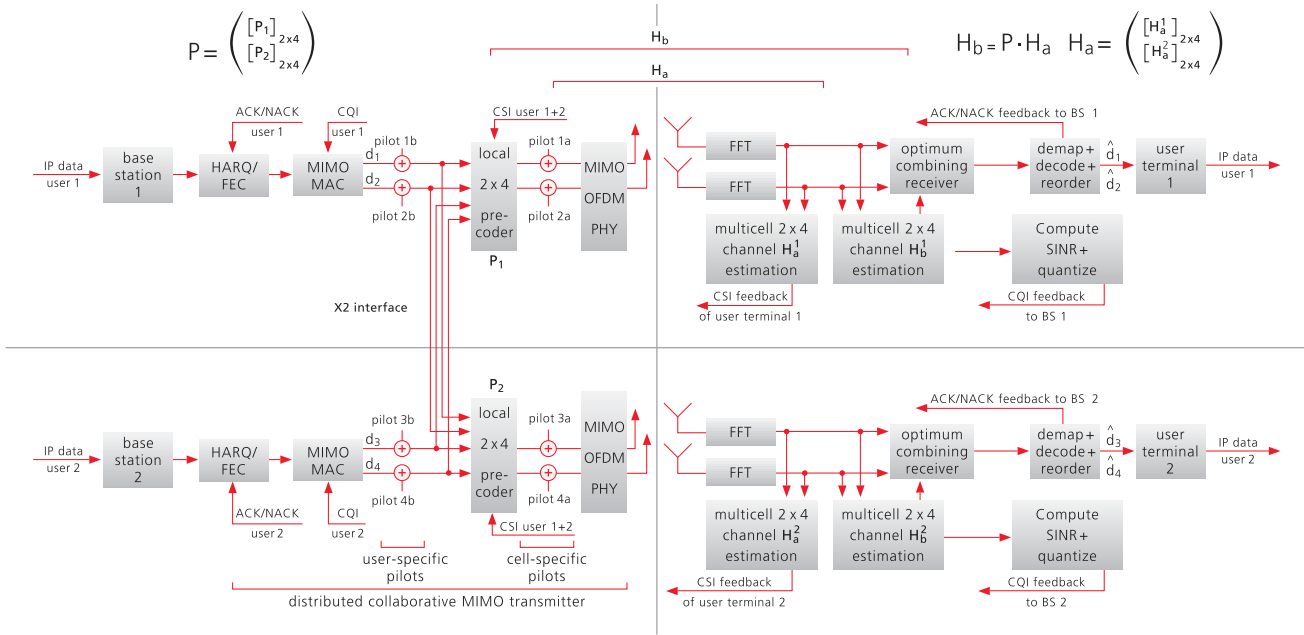


Figure 5. Principle of the experimental CoMP downlink.

Orthogonal sequences are needed, for instance the rows of a 6x6 DFT matrix. Each sequence identifies one stream at a site and it is fed through the precoder. IDFT of the samples on pilot resource elements on the same subcarrier would then separate the channel coefficients for all streams.

For identifying the sites in the second step, we multiply all pilots in a slot by the same chip of a binary sequence taken from a Hadamard matrix. This approach is known as virtual pilots. The terminal performs correlation over multiple slots to separate the pilot signals from different sites. The sequence assignment is shown in Fig. 4, right (see [21]). The hexadecimal numbers encode the rows of a 16x16 Hadamard matrix.

IV. REAL-TIME IMPLEMENTATION

A. Hardware

While the distributed CoMP concept due to the enabling features increases the functional and protocol complexity compared to LTE Release 8, numerical complexity is increased by precoding at the BS and optimum combining at the terminal. We assume that the set of BS involved in the CoMP link is known and all the feedback and X2 links needed have been established.

CoMP has been implemented by modifying an existing LTE trial system in a setup with two BS and two terminals having 2 antennas each. System parameters are given in Table 1. The down-link is capable of single stream and multi stream transmission. The transmission mode as well as the modulation can be set adaptively according to the channel quality identifier (CQI) feedback provided by the terminals in 16 blocks of 75 sub-carriers each. Link adaptation functionality has been maintained in our trials for measuring the throughput. For details, refer to [22].

B. New Functions at the LTE Base Station

Our schematics is shown in Fig. 5. Both terminals are usually served in their cells via co-channel transmission. Data for the terminals are received at the serving BS over S1 realized by 1 Gbit/s Ethernet. Transmission using the internet protocol (IP) is made transparent. Terminals are identified by the IP address. After passing the data through the corresponding queue and hybrid automatic repeat request (HARQ) processors, variable-length transport blocks are formed and fed through FEC and interleaving. Finally, data are mapped onto the RBs.

Next we have inserted precoded pilots as DM-RS (refer to pilot1b...4b in Fig. 5). The design is similar to Fig. 4, center. Pilot spacing is 4 sub-carriers. Antenna- and cell-specific Hadamard sequences of length 4 are used to identify the streams in both cells. Site specific sequences have not been implemented. After this stage in the transmission chain, we have also implemented the synchronous data exchange. Exchange is realized over a separate 1 Gbit/s Ethernet link between the BSs. Transmitted data are packed symbol-wise into Ethernet packets. In the header we transmit a specific mask indicating on which RBs the CoMP mode is used. Since data are transmitted only for these RBs the backhaul is reduced

Table I
REAL-TIME SYSTEM PARAMETERS

Parameter	Value
Up-/Downlink Frequency	2.53/2.68 GHz
Bandwidth	20 MHz each
Number of cells	2
Number of BS antennas	2
Number of terminals	one in each cell
Number of terminal antennas	2
Feedback rate	5 Mbit/s in each cell
X2 data rate (two ways)	≈ 300 Mbit/s

further. Own and foreign data arrive synchronously at the input of the precoder. The added latency due to synchronous data exchange is 0.5 ms using an Ethernet cable link between BS.

Afterwards, the CSI-RS are inserted, denoted as pilot1a...4a in Fig. 5. The design is taken from Fig. 2, center. We have used again Hadamard sequences of length 4 over the first 4 OFDM symbols in the first slot of a radio frame. The same correlation circuit as for the DM-RS can so be reused. Just another subcarrier and sequence mask is applied at the output. Precoded data, DM-RS as well as CSI-RS are finally passed to the MIMO-OFDM physical layer and transmitted over the air.

C. New Functions at LTE Terminals

We have integrated a separate DSP for the multi-cell CSI feedback. The DSP has access to the correlation circuit as well as to a dedicated 100 Mbit/s Ethernet port. The CSI is passed from the down-link receiver into the data path of the up-link transmitter as IP multicast traffic. The CSI feedback is terminated at the precoding DSP in each base station.

By using a standard network technology the multiplexing of the CSI with data on the X2 interface is simplified. On the other hand, great care must be taken to synchronize the CSI from multiple terminals prior to assembling the multi-cell multi-user channel matrix at each BS. We have included time stamps, accordingly, and information about the automatic gain control (AGC) at each receive antenna.

In order to limit the feedback overhead, the channel is fed back once in each 10 ms radio frame. In a two-cell CoMP scenario and over 20 MHz bandwidth, feedback of the uncompressed complex-valued CSI for the 2x4 MIMO downlink channel to both BSs requires $(4 \text{ Tx}) \times (2 \text{ Rx}) \times (144 \text{ pilots}) \times (2 \times 16 \text{ bit}) / 10 \text{ ms} = 3.68 \text{ Mbit/s}$. In the initial experiments, no further feedback quantization has been used. However, the feedback has been formatted carrierwise. For each pilot in the comb, the CSI for the entire 2x4 channel matrix is fed back. In this way the feedback can be limited in the frequency domain, e.g. on RBs intended for CoMP transmission.

Next the precoded channel is evaluated at each terminal. For equalization, the common IRC technique has been applied also known as optimum combining [23] based on the DM-RS. It maximizes the signal-to-interference ratio by exploiting knowledge about the cross-talk between the data streams due to CSI quantization and feedback delay in a time variant channel.

V. MULTICELL TRANSMISSION SCHEMES

The received signal vector \mathbf{y} on each resource element may be described as

$$\mathbf{y} = \mathbf{H}\mathbf{P}\mathbf{x} + \mathbf{n} \quad (1)$$

where \mathbf{H} is the multicell multiuser channel matrix, \mathbf{P} the precoder and \mathbf{n} contains the noise at all antennas.

a) *Isolated cells*: This is an upper bound for the performance. The precoder at each BS1 and BS2 are given as \mathbf{P}_1 and \mathbf{P}_2 , respectively. Either BS1 or BS2 are operated in the whole 20 MHz bandwidth.

$$\mathbf{P}_1 = \begin{bmatrix} 1 & 0 & 0 & 0 \\ 0 & 1 & 0 & 0 \\ 0 & 0 & 0 & 0 \\ 0 & 0 & 0 & 0 \end{bmatrix} \quad \mathbf{P}_2 = \begin{bmatrix} 0 & 0 & 0 & 0 \\ 0 & 0 & 0 & 0 \\ 0 & 0 & 1 & 0 \\ 0 & 0 & 0 & 1 \end{bmatrix} \quad (2)$$

b) *Interference limited case*: This setup realizes a 2-cell system without coordination and thus it is a lower bound on the throughput in a system with full frequency reuse. The precoding matrix is given as

$$\mathbf{P} = \begin{bmatrix} 1 & 0 & 0 & 0 \\ 0 & 1 & 0 & 0 \\ 0 & 0 & 1 & 0 \\ 0 & 0 & 0 & 1 \end{bmatrix} \quad (3)$$

Both BS are hence operated over the whole band. At the receiver we apply IRC based on the DM-RS.

c) *CoMP with rank 2 in each cell*: By providing CSI feedback it is possible to perform cross-wise interference cancellation between both cells. Each user provides the whole 2×4 channel matrix \mathbf{H}_a^1 or \mathbf{H}_a^2 . The BSs assemble the compound channel matrix \mathbf{H} , as shown in Fig. 5. We consider spatial zero forcing (ZF) pre-coding [24] by choosing \mathbf{P} as the right-handed Moore-Penrose pseudo-inverse

$$\mathbf{P} = \mathbf{H}^\dagger = \mathbf{H}^H(\mathbf{H}\mathbf{H}^H)^{-1} \quad (4)$$

Depending on the actual channel, a zero forcing precoder causes considerable signal fluctuation normally not present after the constellation mapper. In order to avoid soft clipping, the precoder output has been normalized such that the columns of the matrix do have the same euclidian norm. This means that all beams jointly provided by all BSs get the same power. Moreover, the precoder output amplitude is downscaled by a safety factor of 4 before passing it into the IFFT. After the IFFT, the signal is upscaled by the same factor.

d) *CoMP with rank 1 in each cell*: This mode is useful if the compound channel matrix \mathbf{H} is rank-deficient. A near-optimal solution is multi-user eigenmode transmission (MET), see [14, 25] and references therein. Each user channel, i.e. \mathbf{H}_a^1 and \mathbf{H}_a^2 , is decomposed via Singular Value Decomposition (SVD) yielding $\mathbf{H}_a^{1,2} = \mathbf{U}\mathbf{\Sigma}\mathbf{V}^H$. Each user is served as close as possible to its dominant eigenmode. For user 1 we get

$$\mathbf{H}_a^1 = \mathbf{u}_1^H \mathbf{U}\mathbf{\Sigma}\mathbf{V}^H = \Sigma_1 \mathbf{v}_1^H \quad (5)$$

To reduce computational complexity, we approximate the filter \mathbf{u}_1 by DFT weights. We set e.g. $\mathbf{u}_1 = [1 - i]^T$ assuming equal gain combining at the terminal. BSs now assemble the compound channel based on the effective channel vectors \mathbf{h}_a^1 and \mathbf{h}_a^2 and obtain the precoder \mathbf{P} according to (4) with dimensions 4×2 .

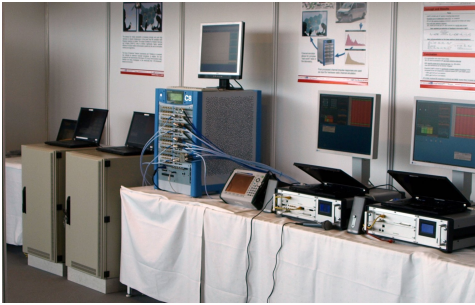
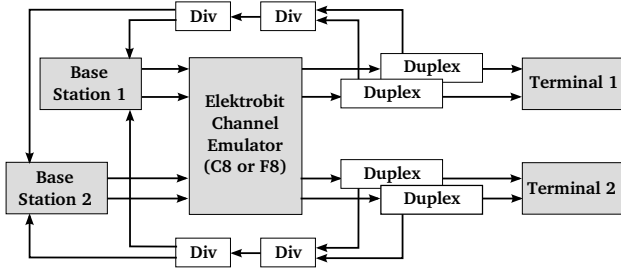
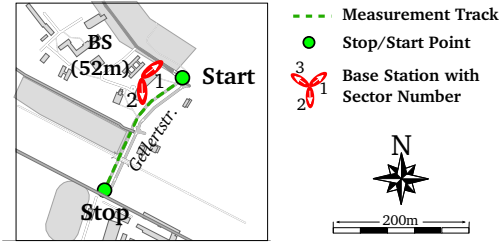


Figure 6. Top: Channel measurement track. Center: Setup in the lab. Bottom: Setup at the ICC 2009.

VI. MULTICELL EXPERIMENTS

A. Measured Channel Data

Network operators increasingly ask for the performance under real-world conditions. We have conducted channel measurements where the multi-cell down-link channels from several base stations have been recorded [26]. Data are used twice, in simulation chains to test the real-world performance of algorithms, and for testing real-time prototypes under field-like conditions. For the measurements we used 20 MHz bandwidth at 2.53 GHz. A real BS site with commercial cross-polarized antennas has been chosen at Lennplatz in the city of Dresden. The map is shown in Fig. 6, top. Two sectors denoted as 1 and 2 are used as a single MIMO transmitter and channels are measured coherently. A particular route with 1.000 snapshots has been selected for each of the two terminals as indicated in the map.

B. Experimental setup

The power levels of signal- and interference links have been modified so that the signal-to-interference ratio at each terminal is monotonously increased as a function of time. Major taps of the multi-path MIMO channel have been extracted and read into the Elektrobit realtime MIMO channel emulator. C8

and F8 models have been used in our labs. The schematics and the setup shown at ICC 2009 are depicted in Fig. 6, center and bottom.

C. Measurement Results

Fixed multi-cell transmission modes (see Section V) have been investigated. Throughput has been measured for a mixture of pseudo random and IP data. Throughput results represent the so-called good-put, i.e. the rate of error-free data bits achieved using an uncoded bit error rate target of 0.025 in the link adaptation. Along the measurement tracks, the mean signal to interference ratio (SIR) for 50 channel snapshots has been evaluated. For each transmission mode, the throughput has been averaged in this time window. Mean throughput has been plotted versus mean SIR at each terminal in Fig. 7.

In the interference-limited scenario (denoted as IRC in Fig. 7) terminal 1 is in a critical scenario partly limited also by the noise. A measurable throughput can be realized with IRC only at $\text{SIR} > 10$ dB. In the SIR range below 10 dB, CoMP can still achieve substantial throughputs which indicates the benefit at the cell edge where similar situations may be typical. With rising SIR, the throughput with CoMP using rank 1 per cell saturates while rank 2 transmission is not preferable for the terminal in this particular situation.

The second terminal is mostly limited by interference. It achieves significant throughput using IRC at $\text{SIR} > 2$ dB already, but the throughput using CoMP is much higher in general. For CoMP with rank 2 per cell, terminal 2 indicates some saturation of the throughput at very high $\text{SIR} > 20$ dB. This is attributed to the time variance of the channel not yet compensated by prediction in our implementation. For terminal 2, we observe that CoMP with rank 2 per cell is preferable compared to CoMP with rank 1 per cell at an SIR above 15 dB, approximately. This reminds us to recent observations in single-cell multiuser MIMO systems, where multi-stream transmission becomes more likely than single-stream above an SNR of 15 dB [22]. Multi-stream becomes more likely at SNR values even below 0 dB if there are 10 users in a cell.

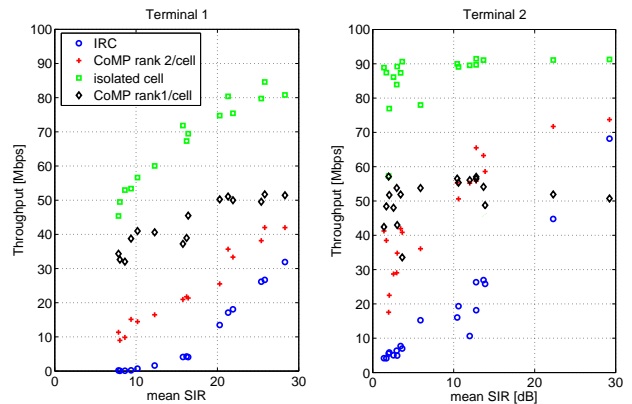


Figure 7. Measured throughput of both terminals in both cells.

The results in Fig. 7 represent first measurement results using downlink CoMP in a particular macro-cell scenario with a single user per cell. The influence of different channel and interference situations will be investigated in further research.

CONCLUSIONS

We have implemented for the first time CoMP transmission in real-time in the FDD downlink. We have significantly reduced the backhaul requirements using a distributed implementation, compared to the centralized approach. On the other hand, the distributed approach requires tight synchronization between the BSs. We have tested CoMP transmission in a multi-cell scenario based on measured outdoor channels. In our experiments it has been observed that terminals served by a CoMP transmission do almost always realize a higher data rate compared to interference-limited transmission. Already with a simple linear CoMP precoder, a significant fraction of the capacity in an isolated cell has been realized while facing substantial inter-cell interference.

ACKNOWLEDGMENTS

The authors wish to thank W. Zirwas, M. Schubert and T. Weber for a fruitful discussions. The German Ministry of Education and Research (BMBF) is acknowledged for financial support of the project EASY-C under contract number 01BU0631.

REFERENCES

- [1] P. Baier, M. Meurer, T. Weber, and H. Troger, "Joint transmission (JT), an alternative rationale for the downlink of time division CDMA using multi-element transmit antennas," *Proc. IEEE ISSSTA '00*, 2000.
- [2] S. Shamai and B. Zaidel, "Enhancing the cellular downlink capacity via co-processing at the transmitting end," *Proc. IEEE VTC '01 Spring*, vol. 3, pp. 1745–1749, 2001.
- [3] T. Weber, I. Maniatis, A. Sklavos, Y. Liu, E. Costa, H. Haas, and E. Schulz, "Joint transmission and detection integrated network (JOINT), a generic proposal for beyond 3G systems," *Proc. ICT'02*, vol. 3, pp. 479–483, 2002.
- [4] A. Goldsmith, S. Jafar, N. Jindal, and S. Vishwanath, "Capacity limits of MIMO channels," *IEEE J. Sel. Areas Commun.*, vol. 21, no. 5, pp. 684–702, June 2003.
- [5] H. Huang and S. Venkatesan, "Asymptotic downlink capacity of coordinated cellular networks," *Proc. ACSSC '04*, vol. 1, pp. 850–855, 2004.
- [6] H. Zhang and H. Dai, "Cochannel interference mitigation and cooperative processing in downlink multicell multiuser MIMO networks," *EURASIP JWCN*, vol. 2004, no. 2, pp. 222–235, 2004.
- [7] G. Foschini, H. Huang, K. Karakayali, R. Valenzuela, and S. Venkatesan, "The value of coherent base station coordination," *Proc. CISS '05*, 2005.
- [8] M. Karakayali, G. Foschini, and R. Valenzuela, "Network coordination for spectrally efficient communications in cellular systems," *IEEE Wireless Commun. Mag.*, vol. 13, pp. 56–61, 2006.
- [9] V. Jungnickel, S. Jaeckel, L. Thiele, L. Jiang, U. Krüger, A. Brylka, and C. Helmolt, "Capacity measurements in a cooperative multicell MIMO network," *IEEE Trans. Veh. Technol.*, vol. 58, no. 5, pp. 2392–2405, 2009.
- [10] TR 36.814 V1.0.0, "Evolved universal terrestrial radio access (e-utra); further advancements for e-utra physical layer aspects," Feb 2009.
- [11] W. Zirwas, J. H. Kim, V. Jungnickel, M. Schubert, T. Weber, A. Ahrens, and M. Haardt, *Distributed Antenna Systems*. Auerbach, 2007, ch. 10, Distributed Organization of Cooperative Antenna Systems, pp. 279–311.
- [12] V. Jungnickel, L. Thiele, M. Schellmann, T. Wirth, W. Zirwas, T. Haustein, and E. Schulz, "Implementation concepts for distributed cooperative transmission," *Proc. ACSSC '08*, oct 2008.
- [13] W. Zirwas, W. Mennerich, M. Schubert, L. Thiele, V. Jungnickel, and E. Schulz, *Cooperative Transmission Schemes*. CRC Press, Taylor and Francis Group, 2009.
- [14] L. Thiele, T. Wirth, T. Haustein, V. Jungnickel, E. Schulz, , and W. Zirwas, "A unified feedback scheme for distributed interference management in cellular systems: Benefits and challenges for real-time implementation," *Proc. EUSIPCO'09*, 2009.
- [15] R. Mudumbai, G. Barriac, and U. Madhow, "On the feasibility of distributed beamforming in wireless networks," *IEEE Trans. Wireless Commun.*, vol. 6, pp. 1754–1763, 2007.
- [16] S. Venkatesan, H. Huang, A. Lozano, and R. Valenzuela, "A WiMAX-based implementation of network MIMO for indoor wireless systems," to appear in *Eurasip Journal on Advances in Signal Processing, Special issue on "Multiuser MIMO transmission with limited feedback, cooperation, and coordination"*.
- [17] V. Jungnickel, T. Wirth, M. Schellmann, T. Haustein, and W. Zirwas, "Synchronization of cooperative base stations," *Proc. IEEE ISWCS '08*, pp. 329 – 334, oct 2008.
- [18] V. Jungnickel, K. Manolakis, L. Thiele, T. Wirth, and T. Haustein, "Handover sequences for interference-aware transmission in multicell MIMO networks," *Proc. WSA'09*, feb 2009.
- [19] M. Sternad and D. Aronsson, "Channel estimation and prediction for adaptive OFDM downlinks," *Proc. IEEE VTC '03 Fall*, pp. 1283–1287, 2003.
- [20] S. Schiffermüller and V. Jungnickel, "Practical channel interpolation for OFDMA," *Proc. IEEE Globecom '06*, 2006.
- [21] L. Thiele, M. Schellmann, S. Schiffermüller, and V. Jungnickel, "Multi-cell channel estimation using virtual pilots," *Proc. IEEE VTC '08 Spring*, May 2008.
- [22] V. Jungnickel, M. Schellmann, L. Thiele, T. Wirth, T. Haustein, O. Koch, E. Zirwas, and E. Schulz, "Interference aware scheduling in the multiuser MIMO-OFDM downlink," *IEEE Commun. Mag.*, June 2009.
- [23] J. H. Winters, "On the capacity of radio communication systems with diversity in a rayleigh fading environment," *IEEE J. Sel. Areas Commun.*, vol. 5, no. 5, pp. 871–878, June 1987.
- [24] Q. H. Spencer, A. Swindlehurst, and M. Haardt, "Zero-forcing methods for downlink spatial multiplexing in multiuser MIMO channels," *IEEE Trans. Signal Process.*, vol. 52, no. 2, pp. 461–471, 2004.
- [25] F. Boccardi, H. Huang, and M. Trivellato, "Multiuser eigenmode transmission for mimo broadcast channels with limited feedback," *Proc. IEEE SPAWC'07*, June 2007.
- [26] S. Jaeckel, L. Thiele, A. Brylka, L. Jiang, and V. Jungnickel, "Intercell interference measured in urban areas," *Proc. IEEE ICC'09*, 2009.